TECHNICAL REPORT ARSCD-TR-79008

SINTERING CYCLE INFLUENCE ON P/M STEEL FORGINGS' DYNAMIC PROPERTIES

ANDREW CROWSON

AUGUST 1979

US ARMY ARMAMENT RESEARCH AND DEVELOPMENT COMMAND
FIRE CONTROL AND SMALL CALIBER
WEAPON SYSTEMS LABORATORY
DOVER, NEW JERSEY

The views, opinions, and/or findings contained in this report are those of the author(s) and should not be construed as an official Department of the Army position, policy or decision, unless so designated by other documentation.

Destroy this report when no longer needed. Do not return it to the originator.

The citation in this report of the names of commercial firms or commercially available products or services does not constitute official endorsement or approval of such commercial firms, products, or services by the United States Government.

REPORT DOCUMENTATION PAGE

READ INSTRUCTIONS BEFORE COMPLETING FORM

1. REPORT NUMBER: Technical Report ARSCD-TR-79008
2. GOVT ACCESSION NO.:
3. RECIPIENT'S CATALOG NUMBER:

4. TITLE (and Subtitle): Sintering Cycle Influence on P/M Steel Forgings' Dynamic Properties

5. TYPE OF REPORT & PERIOD COVERED: Final

6. PERFORMING ORG. REPORT NUMBER:

7. AUTHOR(s): Andrew Crowson

8. CONTRACT OR GRANT NUMBER(s):

9. PERFORMING ORGANIZATION NAME AND ADDRESS:
ARRADCOM, FC&SCWSL
M&MT Division (DRDAR-SCM-P)
Dover, New Jersey , 07801

10. PROGRAM ELEMENT, PROJECT, TASK AREA & WORK UNIT NUMBERS:
DA Project 1T162105AH84
AMCMS Code: 612105.11. H8400

11. CONTROLLING OFFICE NAME AND ADDRESS:
ARRADCOM, TSD
STINFO (DRDAR-TSS)
Dover, NJ 07801

12. REPORT DATE: AUGUST 1979

13. NUMBER OF PAGES: 31

14. MONITORING AGENCY NAME & ADDRESS (if different from Controlling Office):

15. SECURITY CLASS. (of this report): Unclassified

15e. DECLASSIFICATION/DOWNGRADING SCHEDULE:

16. DISTRIBUTION STATEMENT (of this Report)

Approved for public release; distribution unlimited.

17. DISTRIBUTION STATEMENT (of the abstract entered in Block 20, if different from Report)

18. SUPPLEMENTARY NOTES

19. KEY WORDS (Continue on reverse side if necessary and identify by block number)

Prealloyed steel powders
Sintering
P/M forging
Dynamic properties

20. ABSTRACT (Continue on reverse side if necessary and identify by block number)

The effects of sintering environments and their respective parameters on the dynamic properties of P/M steel forgings have been determined. Compacted preforms were sintered from 10 to 90 minutes over a range of temperatures (1100-1370°C) in inert, vacuum, and reducing atmospheres. The final oxide content was found to vary exponentially with sintering time, sintering temperature, and gas flow-rate regardless of the type of

atmosphere used. Reduction of the metal oxides was basically controlled by two factors: (1) carbon and (2) elevated temperature. Two levels of oxide reduction were evident. The initial level involved a reduction of the majority of the metal oxides (iron, molybdenum, and nickel oxides), whereas the secondary level resulted in a slow reduction of the more thermodynamically stable oxides of manganese and chromium. Elongation, reduction in area, and impact energy values showed a corresponding increase with decreasing oxide content. Forgings with oxide contents above 500 ppm possessed surface as well as internal oxides, thereby contributing to early failure due to ease of crack propagation. Fracture toughness values were established at two discrete levels depending on whether ductile or brittle fracture occurred. Ductile/brittle fracture criteria were correlated with the final oxide content.

TABLE OF CONTENTS

TABLES

FIGURES

INTRODUCTION

Universal acceptance of powder metallurgy (P/M) steel forgings requires attainment of physical and mechanical properties comparable to conventional steel forgings. Almost all of these properties can be obtained by the closing of voids normally present in standard P/M parts in such a manner as to fully densify and achieve a sound metallurgical bond during forging. Significant lateral deformation under high forging temperature and pressure is required to achieve such an effect (ref 1). Full density P/M steel forgings with tensile and yield strengths similar to conventional forgings can be easily obtained under these conditions (ref 2-4). However, equivalent dynamic properties of ductility, impact, and fatigue are more difficult to achieve.

The major factor affecting these properties is the nonmetallic inclusions unfavorably distributed throughout the fully dense P/M structure (ref 5-6). These inclusions are associated with the surface and internal oxides formed during the P/M forging process.

Oxidation during the P/M forging process can occur in three ways:

1. Oxide scale can form on the perform surface;

2. Oxides can form on the internal surface of the preform, and

3. Selective oxidation of the alloying elements can occur in the powder and the preform.

Oxide scale, or surface oxides, can form on a preform during exposure to air either when transferred from a furnace to a die or when processed in a nonprotective furnace. When the surface is oxidized in such a manner, the underlying metal may also be decarburized. Internal scale, or oxide formation, can take place because the preform is porous. This type of oxidation can occur when the hot preforms are exposed to air or even in a "protective" atmosphere, if proper precautions are not taken. Proper precautions include maintaining a sufficiently low dew point, eliminating air leaks into the furnace, and eliminating condensation in the cooling zone.

Selective oxidation of the alloying elements may occur at any stage of the entire P/M forging process. Selective oxidation is defined as the oxidation of alloying elements in preference to iron, and it may occur during manufacture of the powder, during sintering of the preform, or during exposure of the hot preform to air during transfer to the forging die (ref 7). Elements such as chromium, manganese, vanadium, boron, and others are much less noble than iron and will oxidize when the iron will not. When the iron oxides are subsequently reduced, the oxides of these less noble metals may not be reduced.

Achievement of acceptable dynamic properties in P/M forgings requires elimination, or a major reduction, of the above types of oxides (ref 8 and 9). Approaches used to achieve this elimination or reduction reflect the theme of a large body of research in powder metallurgy. Previous studies have shown that the sintering cycle of the P/M forging process is the most amendable step to accomplish this goal (ref 9). Because of the importance of the sintering cycle, the current investigation was conducted to establish the effects of sintering environments and their respective parameters (time, temperature, and dew point) on P/M steel forged properties. The results obtained in this study, as with prior years' efforts, will be used toward developing capabilities in P/M forgings which meet the unique requirements of military applications.

EXPERIMENTAL PROCEDURE

Commercially available 4600 steel powder was used in this investigation. The chemical composition of the powder is shown in table 1 along with the chemical analysis required by AISI specification for wrought 4600 metal. The powder was modified (lower manganese, higher molybdenum) ostensibly to promote processing conditions. Flake graphite was then added to the powder to obtain a 0.4 percent carbon content.

The blended powder was compacted into 8.9 cm X 1.9 cm rectangular bars to a 80 percent theoretical density with the use of a graphite die, wall-spray lubricant. The compaction operation was conducted in a closed, confined die and a Riehle 205,000 kg tensile testing machine. Spring inserts in the bottom of the die assembly enabled the compaction operation to simulate a double-acting press, thus yielding uniform density profiles in the compacts. The compacted preforms were sintered either in a vacuum, an argon, or a hydrogen atmosphere at temperatures in the range of 1090°C-1315°C for times of

Table 1. Chemical analysis of 4600 prealloyed powder

Element	AISI Specification %	4600 Powder %
Carbon	-	-
Nickel	1.65 - 2.00	1.77
Molybdenum	0.2 - 0.3	0.48
Manganese	0.6 - 0.8	0.23
Copper	-	0.05
Chromium	-	0.05
Phosphorus	0.04 Max	0.01
Sulfur	0.04 Max	0.02
Silicon	0.02 - 0.34	0.07
Oxygen	-	0.152

10 to 90 minutes. Vacuum sintering was conducted in a Brew vacuum furnace at 10^{-4} to 10^{-5} torr, whereas argon and hydrogen sintering were preformed in a batch sintering furnace equipped with a 14 cm X 19 cm X 61 cm Inconel muffle. Gas flow-rates of 2800 to 14,000 cc/min were used for the argon and hydrogen sintering.

After sintering, the heated preforms were transferred directly to a preheated (150°C - 230°C) closed-forging die and forged at 550MPa to achieve full densification. The dimensions of the forging die were such that a minimum amount of lateral deformation occurred during the forging operation. The forgings were subsequently austenitized at 843°C for 1/2 hour and tempered at 621°C for one hour to achieve a Rockwell C 30-33 hardness.

Characterization of the forged specimens included the determination of oxide content, elongation, reduction in area, impact energy, and fracture toughness. Metal oxide content was measured as oxygen by use of vacuum fusion analysis; elongation and reduction in area was determined by standard R2 tensile bars (ASTM); and impact testing was performed on an instrumented impact machine. The load-time (deflection) curves obtained enabled a determination of additional information related to yielding, fracture, ductility, and crack propagation.

RESULTS AND DISCUSSION

Powder

The powder characteristics for the 4600 steel powder used are shown in table 2. A bimodal particle size distribution was found present with an apparent density of 2.99 g/cm^3 and a flow rate of 25.8 sec. Individual powder particles evaluated by scanning electron microscopy (SEM) and standard optical metallography are shown in figure 1. SEM examinations showed that the particles consisted of a distribution of spherodial to popcorn-like shapes. Metallographic examinations also showed that the microstructure of the particles had a generally uniform grain size of ASTM No. 12.

Sintering

The residual oxide content in the sintered preform as a function of gas flow-rate, sintering time, and sintering temperature was determined in a variety of sintering atmospheres. Final oxide content was used as the limiting criteria due to its strong influence on impact

Table 2. Characteristics of 4600 prealloyed powder

U.S. Screen size [a]	Sieve analysis, wt%
+80 (180μ)	0.1
-80 +100	4.5
-100 +140	14.5
-140 +200	23.4
-200 +230	7.5
-230 +325	18.7
-325 (44μ)	31.3
Apparent density [b] (g/cm^3)	2.99
Flow rate [c] (sec)	25.8

[a] Measured in accordance with ASTM B-214-56.
[b] Measured in accordance with ASTM B-212-48.
[c] Measured in accordance with ASTM B-213-48.

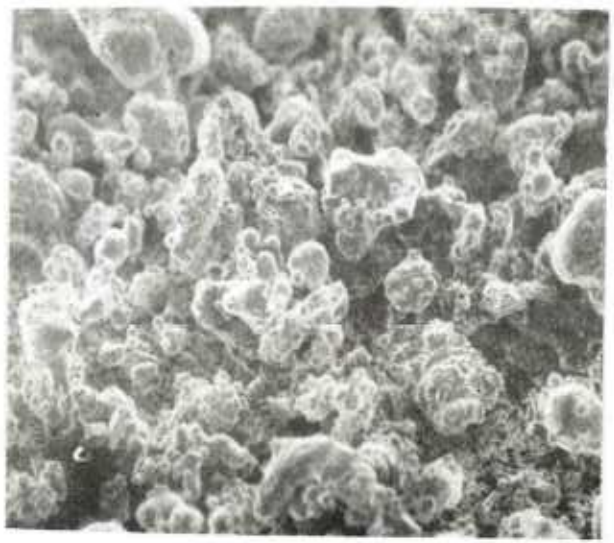

80X

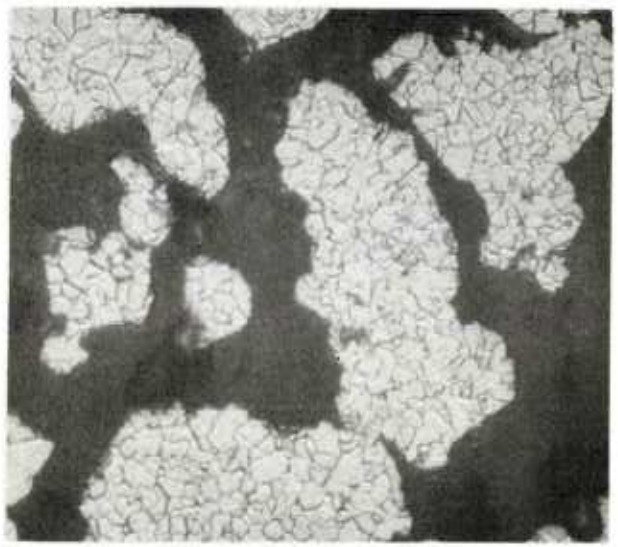

Nital Etch 400X

Figure 1. Particle shape and microstructure of 4600M powder.

and ductility properties in P/M forgings. Similar oxide contents were obtained when the preforms were sintered in argon and hydrogen. In contrast, vacuum sintering resulted in preforms with slightly lower oxide contents.

The effect of sintering temperature on final oxygen content is shown in figure 2. Four preform sintering temperatures (1040°C, 1090°C, 1150°C, and 1200°C) were investigated. Because of the added capability of existing equipment two additional sintering temperatures (1260°C and 1320°C) were investigated for vacuum sintering. A sintering time of 40 minutes was used for all sintering runs, and a gas flow-rate of 8500cc/min was used for hydrogen and argon. The sintering temperature had a significant effect on the preform oxygen content. Oxygen content decreased dramatically as the sintering temperature was increased from 1040°C to 1200°C. The oxygen content was over 1000 ppm at 1040°C, whereas at 1200°C, the oxygen content was below 200 ppm. Higher sintering temperatures of 1260°C and 1320°C produced only a gradual reduction in the oxygen content.

These experiments demonstrated that a variety of atmospheres can be used during the sintering cycle for reduction of the oxide content in P/M steel forgings. A reducing atmosphere, such as hydrogen, is not necessarily an essential requirement for obtaining low oxygen content forgings. An inert or vacuum atmosphere can accomplish similar results. Therefore, reduction of the metal oxides is basically controlled by two factors. They are:

1. Carbon addition

2. Sintering temperature

Reactions describing this reduction process can then be written and combined as follows:

$$2C(s) + O_2(g) \longrightarrow 2CO(g) \qquad (1)$$

$$xM(s) + \frac{y}{2} O_2(g) \longrightarrow M_xO_y(s) \qquad (2)$$

and

$$yC(s) + M_xO_y(s) \longrightarrow yCO(g) + xM(s) \qquad (3)$$

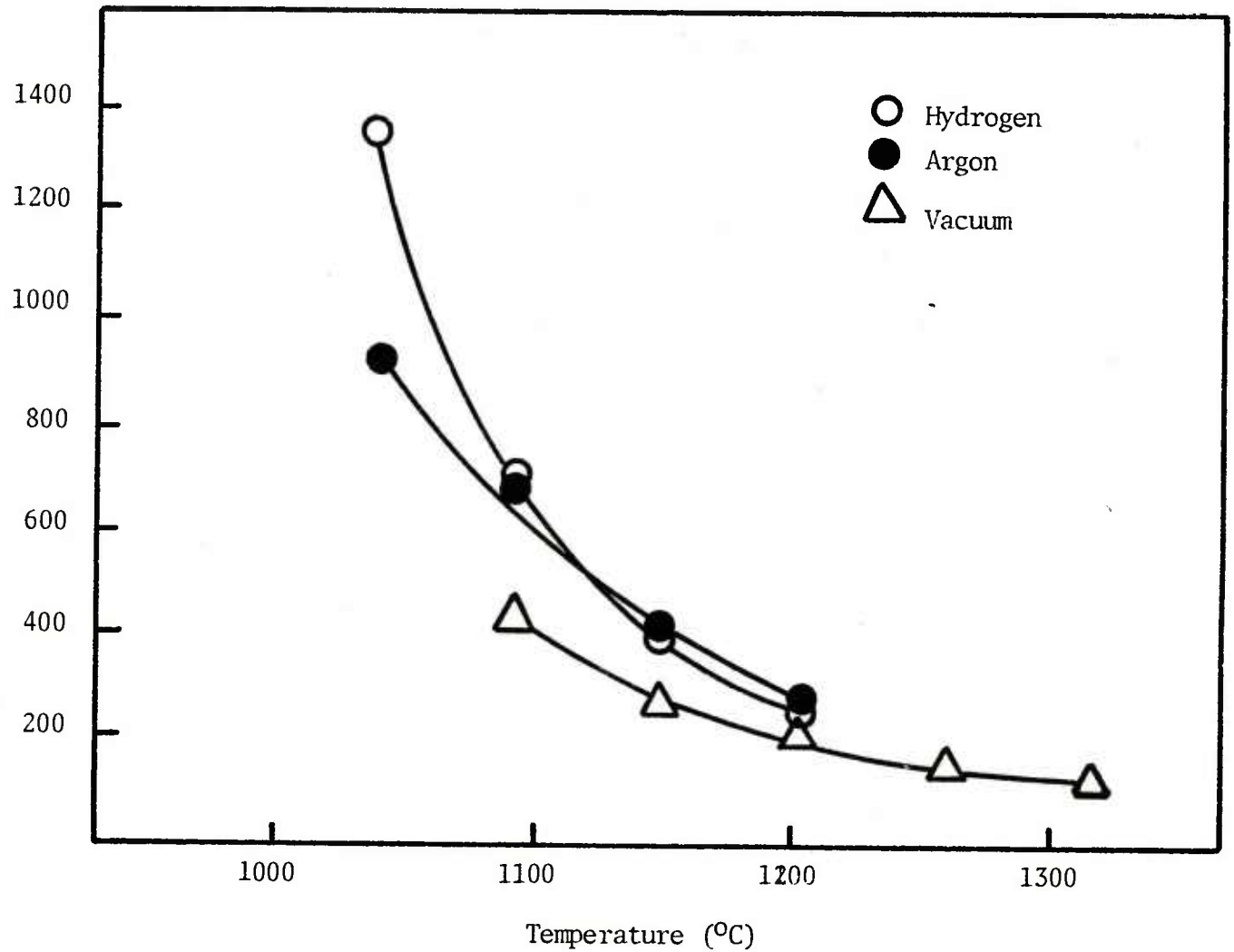

Figure 2. Sintering temperature effect on oxygen content (Sintered for 40 minutes at temperature).

A useful means of interpreting the oxide reduction curves in figure 2 can be accomplished by thermodynamically analyzing the above equations. The free energy of formation (ΔF_o) of a metal oxide will determine whether the oxide will reduce. Since free energy values are dependent upon temperature, the conditions necessary for reduction will vary. The Ellingham Free Energy Chart, shown in figure 3, gives the relative stability of metal oxides as a function of temperature (ref 10). Knowing the type of oxide to be reduced and the reducing environment (equation 1) provides a relatively easy means to predict the temperature necessary for oxide reduction (equation 3).

The oxides reduced in this study were iron, molybdenum, nickel, copper, chromium, and manganese. The first group of oxides (iron, molybdenum, nickel and copper) represents the bulk of the metal oxides present. These oxides are relatively easy to reduce and are found in the upper region (1040°C - 1150°C) of the curves in figure 3. With the use of the Ellingham Free Energy Chart and Equation 3, these oxides can be reduced as low as 815°C. At this point, the CO-ΔF_o curve crosses the FeO-ΔF_o curve. Above this temperature, carbon will reduce pure iron oxide in contact with pure iron. Since nickel, copper, and molybdenum are more noble than iron, they will also be reduced at this temperature. This prediction is made solely on the basis of thermodynamics. In reality, the kinetics at this temperature are very slow. Temperatures in excess of 1090°C were required to reduce these oxides in a reasonable amount of time.

Reduction of the oxides less noble than iron (chromium and manganese) requires more stringent conditions. Their free energy curves are much lower than iron and do not cross the CO-ΔF_o curve until temperatures of 1240°C and 1410°C, respectively, are achieved. Experimentally, however, reduction of these oxides occurs about 1200°C (ref 11). This occurs because the metals are alloyed and in dilute form. Reduction of these oxides is represented by the lower region (1230°C - 1315°C) of the curves in figure 3.

In a second set of experiments, the effect of sintering time on final oxygen content was determined. The results are shown in figure 4. The preforms were sintered at 1200°C; a flow rate of 8500 cc/min was used in the hydrogen and argon gas sintering experiments. As shown, the resultant curves have two levels of oxide reductions. The first, or initial level, shows a dramatic reduction rate of oxide content. This corresponds to the reduction of the iron

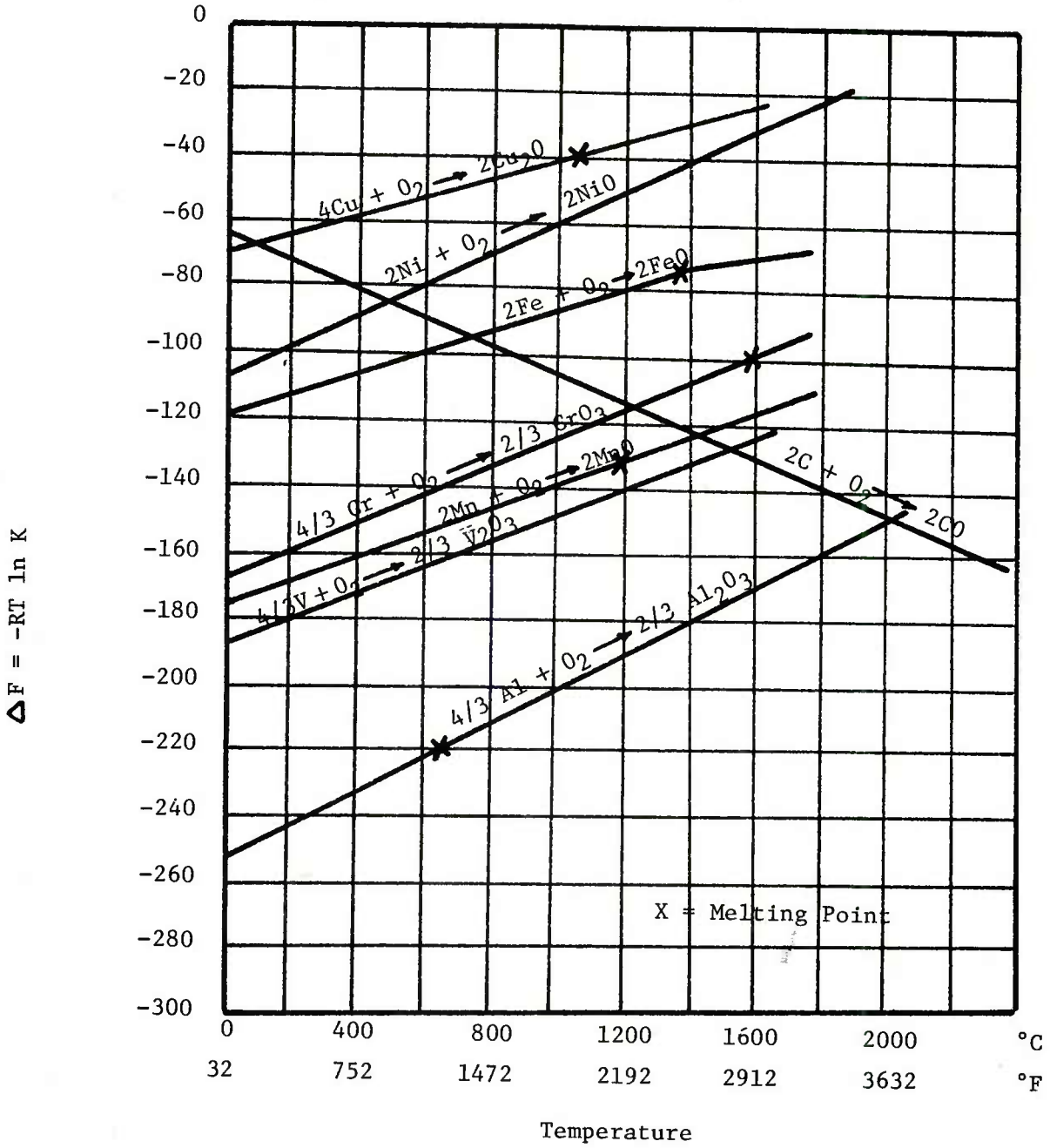

Figure 3. Change in free energy vs. temperature for several reactions.

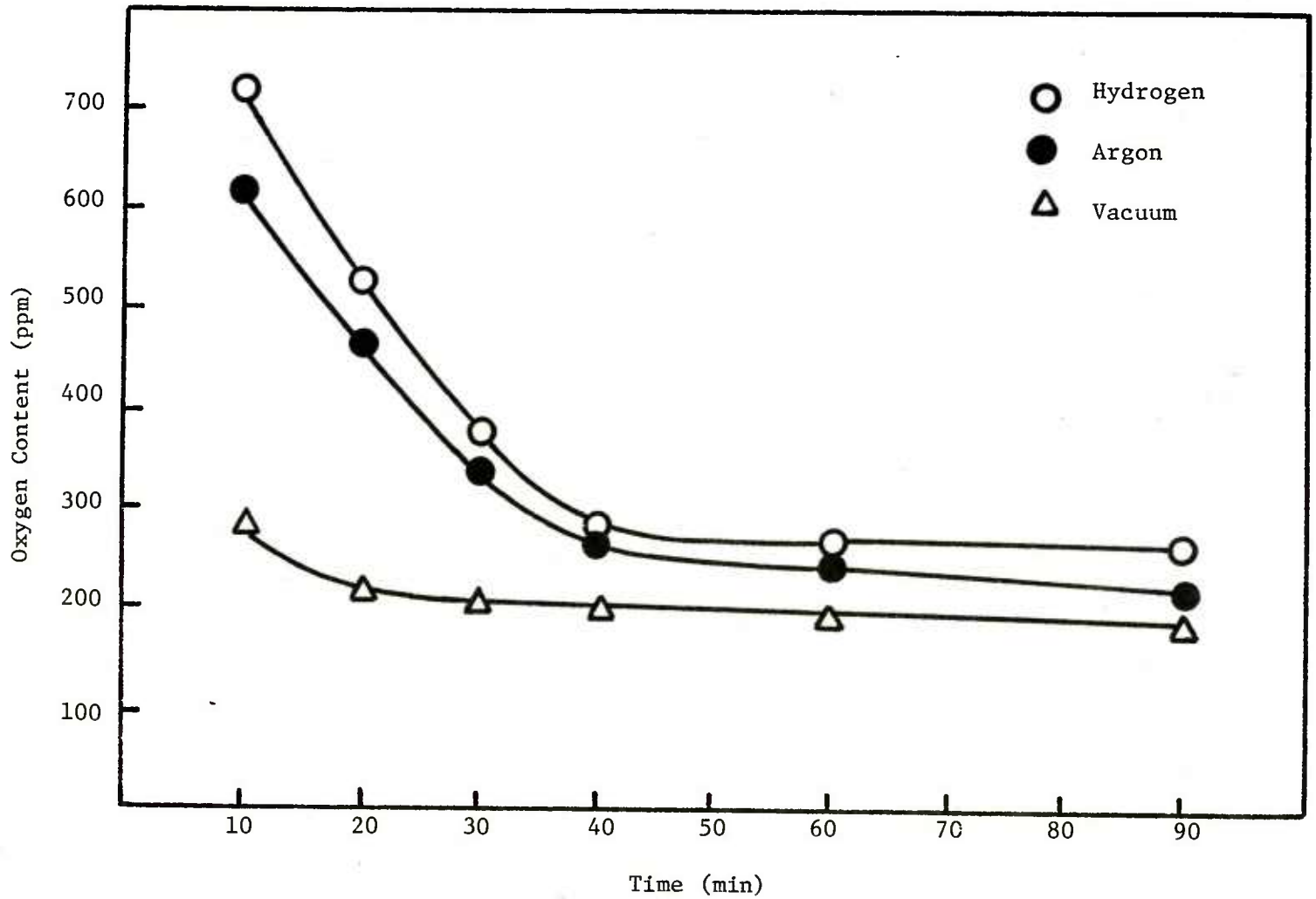

Figure 4. Sintering time effect on oxygen content at 1200°C.

oxides and oxides of the metals more noble than iron. Sintering conditions are such that all these oxides are easily reduced. The second, or final level, shows a slow reduction rate of the remaining oxides. Here the metal oxides less noble than iron are slowly being reduced. The bulk of these oxides correspond to the manganese oxides present in the powder.

Another difference noted in the curves is that of the effect of vacuum sintering. The sintering time is reduced by one-half (20 minutes instead of 40 minutes) during the initial level. Two factors account for this discrepancy: (1) The preheating time necessary to reach 1200°C in a vacuum system has not been taken into account and (2) high dissociation pressures of the respective metal oxides are achieved during vacuum sintering. Either of these factors could substantially influence the initial sintering time interval.

In hydrogen and argon sintering, the gas flow-rate is an additional variable. Gas flow-rates significantly affect the final preform oxygen content as shown in figure 5. The effect of flow rates from 2800 to 14,000 cc/min were evaluated. The preforms were sintered for 40 minutes at 1200°C. As noted from the resultant graph, the final oxygen content in the preforms is decreased dramatically when sintered in increasing gas flow-rates. Increasing the flow rate from 2800cc/min to 14,000 cc/min reduces the oxygen content by one-half. Lowering of the furnace atmospheric dew point and the rapid flushing out of the gaseous oxide products (thus, facilitating the diffusion of carbon monoxide) account for this decrease.

Properties

Since dynamic properties of P/M steel forgings are strongly influenced by oxygen and non-metallic inclusion content, they were used to evaluate the final forgings. Reduction in area, elongation, and impact energy were among the dynamic properties determined. The correlation between the ductility properties and the final oxygen content is shown in figure 6. Elongation and reduction in area values show a corresponding increase with decreasing oxygen content. This interdependence is markedly stronger in the 300 to 1000 ppm oxygen region. Impact energy data relating oxygen content to the forging's impact energy (figure 7) show a similar correlation.

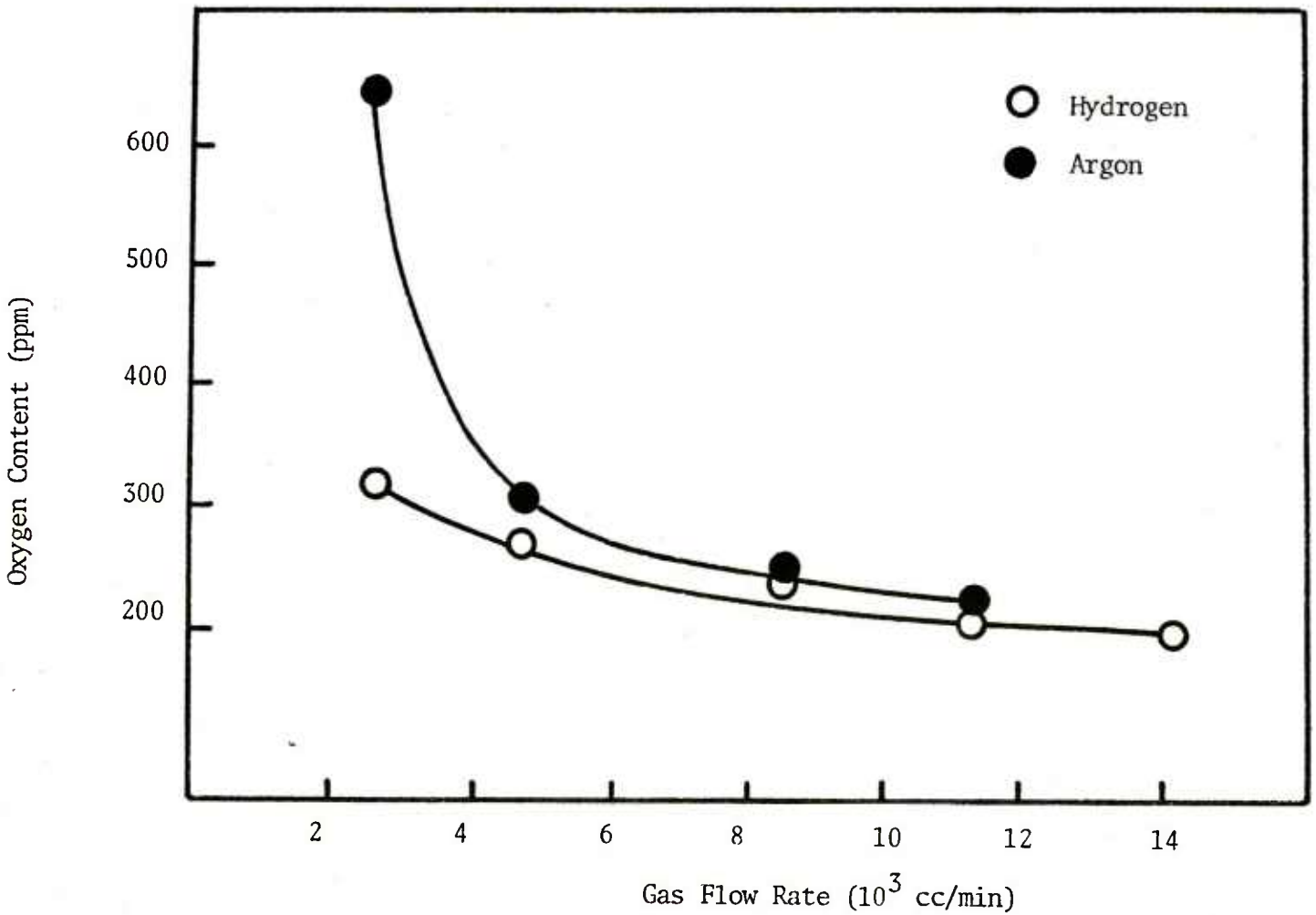

Figure 5. The effect of gas flow-rate on reduction of oxides at 1200°C.

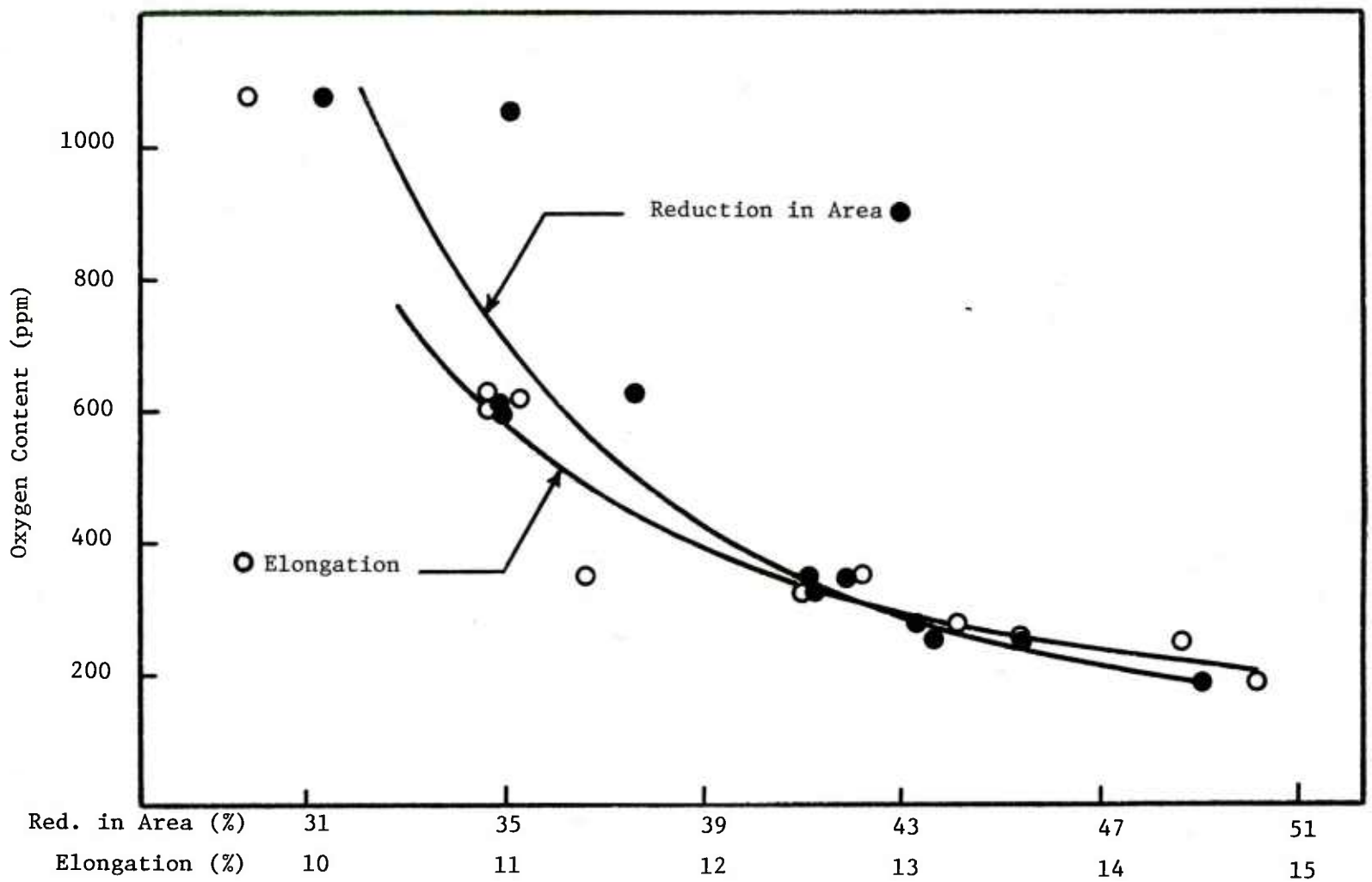

Figure 6. Reduction in area and elongation of P/M steel forgings as a function of oxygen content.

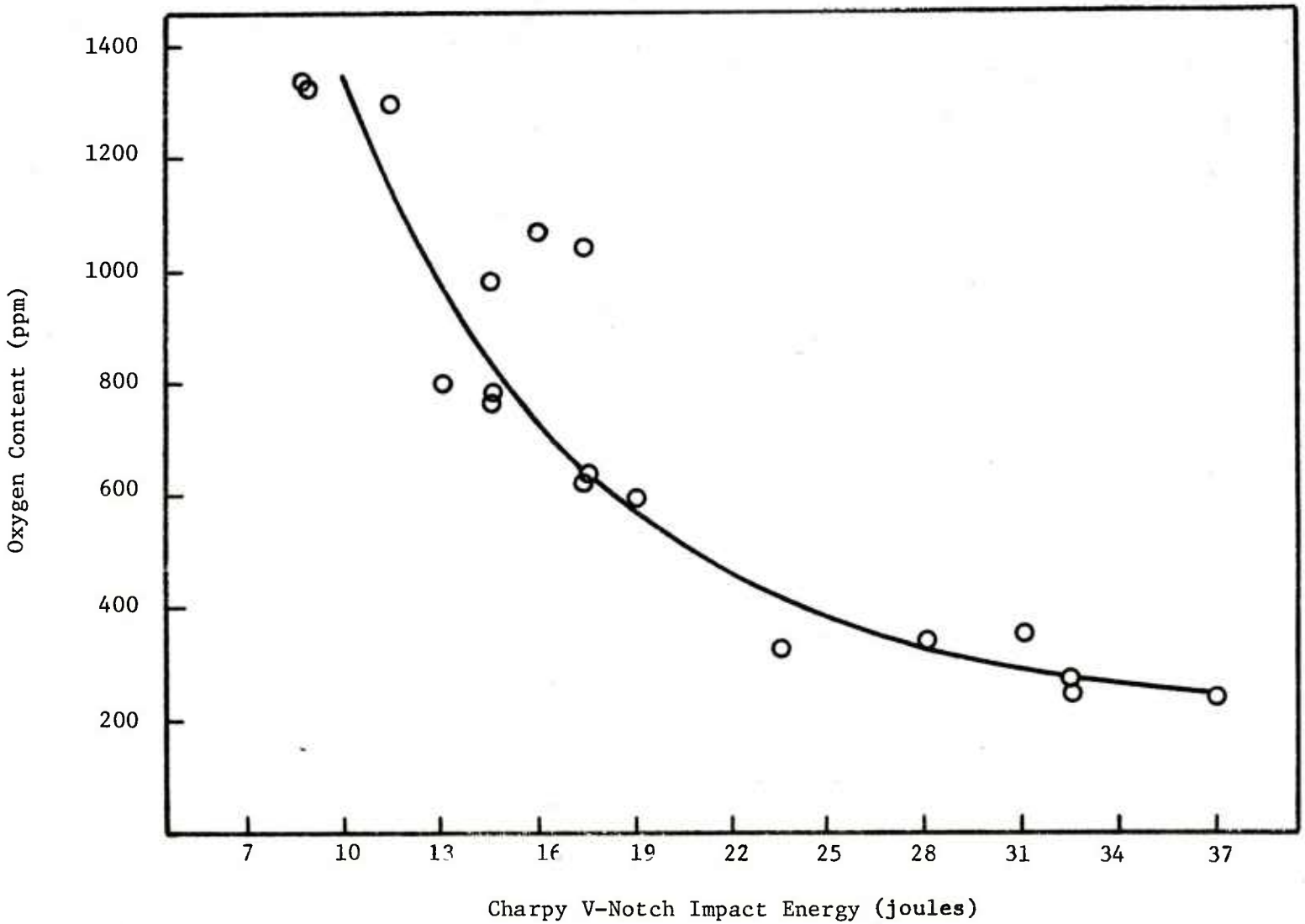

Figure 7. Impact energy of P/M steel forgings as a function of oxygen content.

Previous investigators (ref 12) have postulated that the key to the great influence of the oxygen content on the impact resistance of quenched and tempered hot-formed P/M steels is the morphology of the oxides. This morphology is in turn determined by the type of oxides that are present. Forgings with a low-oxide content contain irreducible internal oxides exclusively. These tend to be rounded, isolated, and well distributed throughout the P/M forging. On the other hand, forgings with a high-oxide content possess surface, as well as internal, oxides that have not been reduced. The unreacted surface oxides are very detrimental to the ductility and impact properties. They tend to form at the particle boundaries during sintering, thereby acting as a kind of perforation in the structure and form an easy path for crack initiation and propagation.

Since fracture toughness is an indication of inhomogeneous defects within a structure, fracture toughness values as a function of oxygen content in the forging were also determined. Measurable parameters from test records of instrumented Charpy impact tests were used with equations available in the literature (ref 13 and 14) and reduced to toughness values. Typical load-load point displacement curves for various oxygen levels are shown in figure 8. The type of curves obtained for P/M steel forgings with high oxygen contents (789 to 1300 ppm) are represented in figures a, b, and c. For these samples, fracture toughness values were determined with the use of the following equations:

$$K_Q = ZP_m \tag{4}$$

$$Z = \frac{1.5Y\ell\, a^{1/2}}{bw^2} \tag{5}$$

$$Y = 1.93 - 3.07\frac{a}{w} + 14.53\left(\frac{a}{w}\right)^2 - 25.11\left(\frac{a}{w}\right)^3 + 25.8\left(\frac{a}{w}\right)^4 \tag{6}$$

where K_Q = fracture toughness ($MPa\sqrt{m}$)
Z = constant
P_m = maximum load (MPa)
ℓ = span length (m)
b = specimen width (m)
w = thickness (m)
a = total crack length (m)

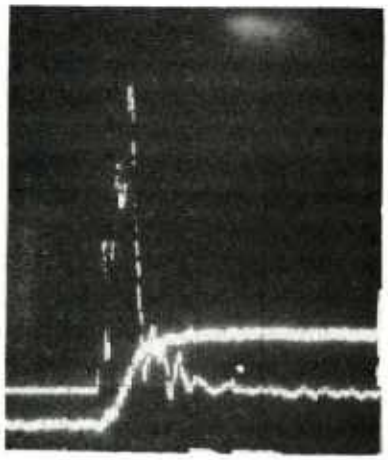

a. 1330 ppm

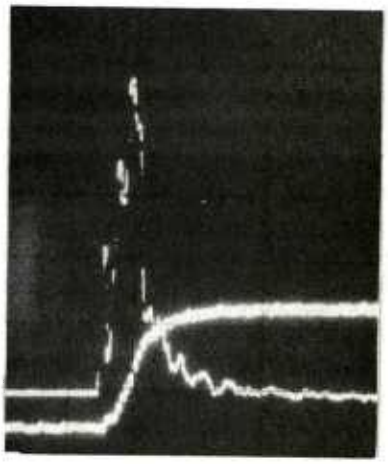

b. 1030 ppm

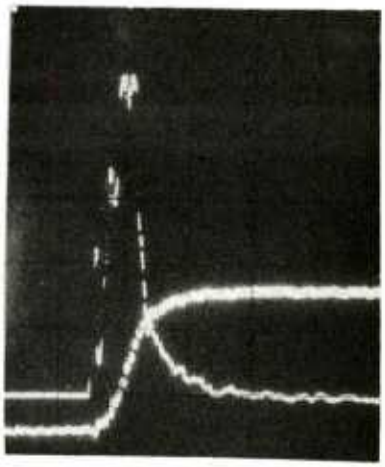

c. 789 ppm

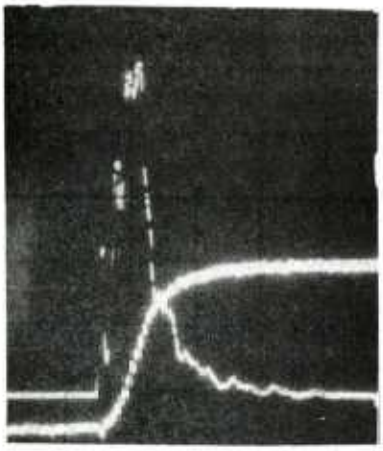

d. 600 ppm

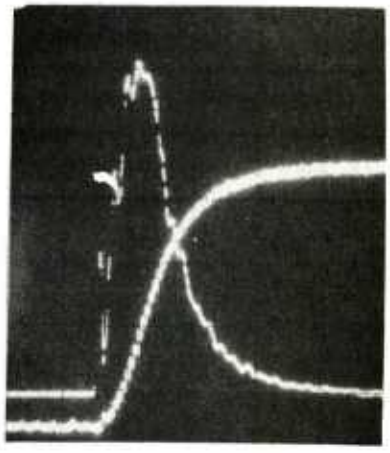

e. 344 ppm

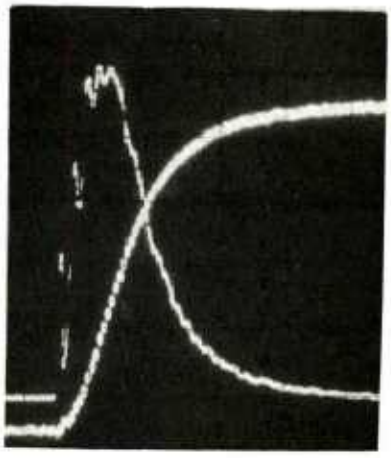

f. 255 ppm

Figure 8. Load-time displacement curves for P/M steel forgings containing various amounts of oxides.

This approach is considered to be the most representative of plane-strain conditions since failure has occurred before material yielding. The calculated fracture toughness values for these specimens as a function of their oxide content is shown in table 3. As expected, a corresponding decrease in K_Q with increasing oxide content is exhibited. Overall, a brittle fracture mode of behavior followed by shear lip formation was indicative for these forgings. The amount of energy required for brittle fracture (W_F), determined from figure 9, was directly related to the oxide content with early failure associated with forgings containing higher oxides.

Typical fracture curves for P/M steel forgings with low oxygen contents (255 to 600 ppm) are represented in figure 8d, e, and f. In these instances, the maximum load is no longer a valid criteria for obtaining plane-strain fracture toughness values since fracture occurs after general yielding and a departure from the linear theory of elasticity occurs. Therefore, the approach used by Wells (ref 15) relating strain energy to crack-opening displacement was employed to calculate fracture toughness values. The equations used in these cases were as follows:

$$K_Q = (G_c\, E)^{1/2} \tag{7}$$

$$G_c = \text{COD}\, 6\, y \tag{8}$$

$$\text{COD} = \frac{\text{LPD}}{\ell/2}\, d \tag{9}$$

where

K_Q = fracture toughness ($\text{MPa}\sqrt{\text{m}}$)

G_c = critical strain energy release rate (MPa·m)

Table 3. Fracture toughness of high oxide content P/M steel forgings

Oxygen (ppm)	W_F (joules)	K_Q ($\text{MPa}\sqrt{\text{m}}$)
789	11.1	98
1030	10.6	89
1330	7.9	87

W_I = crack initiation energy
W_C = crack propagation energy
W_S = shear lip energy
W_F = brittle fracture energy

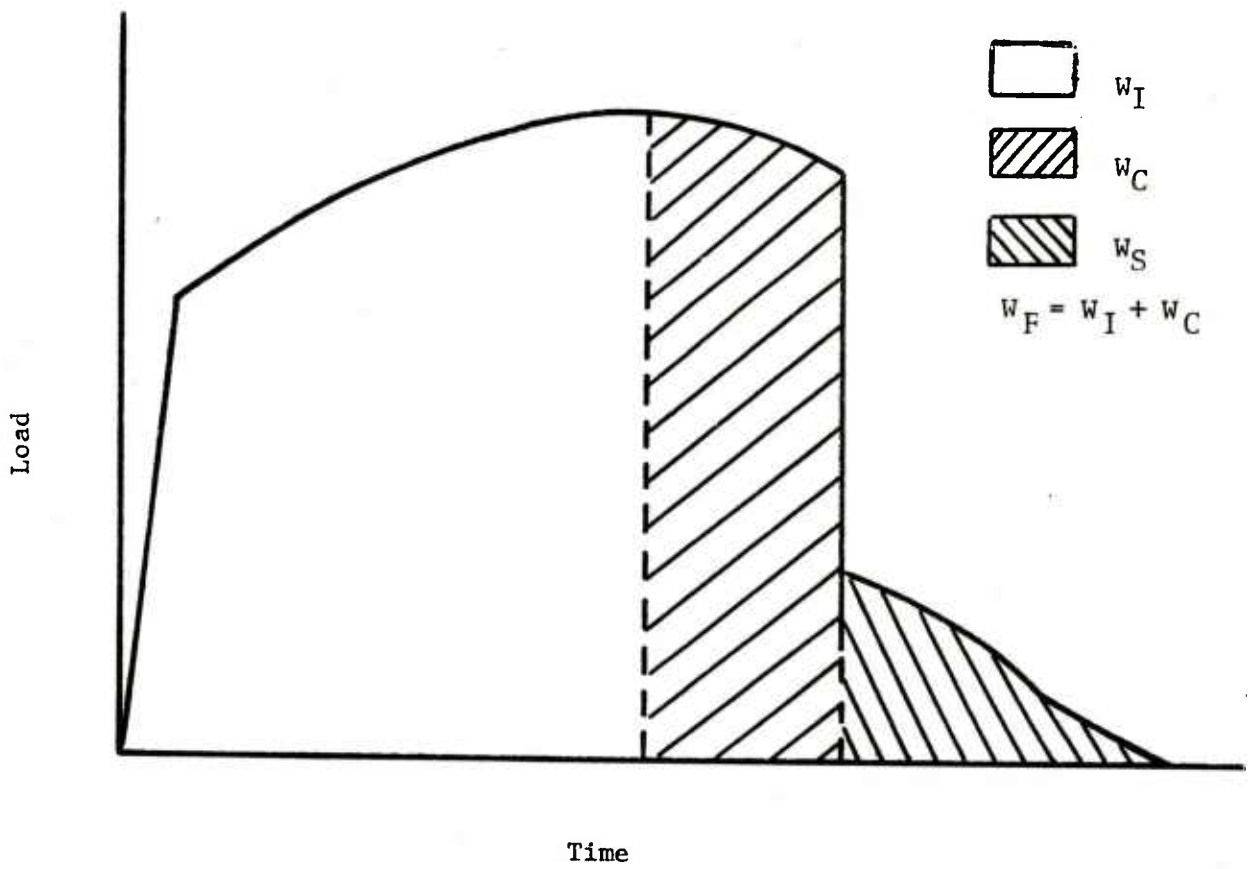

Figure 9. An idealized load-time trace for an impacted charpy V-notch specimen.

Table 4. Fracture toughness of low oxide content P/M steel forgings

Oxygen (ppm)	W_I (joules)	W_C (joules)	W_F (joules)	$K_Q\sqrt{m}$ (MPa$\sqrt{m}$)
225	11.4	14.4	25.8	142
344	10.2	11.7	21.9	134
600	8.5	4.6	13.1	126

E = elastic modulus (MPa)
COD = crack opening displacement (m)
σ_y = yield strength (MPa)
LPD = load point displacement (m)
ℓ = span length (m)
d = depth of axis of rotation (m)

The resultant fracture toughness values as a function of the oxygen contents are shown in table 4. As seen in table 3, a similar trend is noted here. Increasing the oxygen content of the forging results in a decrease in the fracture toughness value. The major difference noted in table 3 forgings and table 4 forgings is the magnitude of K_Q. The additional ductility, as noted from the fracture curves for the low-oxygen content forgings, substantially increases the fracture toughness values. The amount of ductility associated with these forgings can best be seen when the unstable crack propagation energies (W_C), determined from figure 9, are compared. These energies increase proportionally with decreasing oxygen contents. Values range from 4.6 joules for 600 ppm oxide forgings up to 14.4 joules at the 255 ppm level. A similar trend is noted for the crack-initiation energies (W_I), calculated from figure 9, for these forgings.

Fracture of the low-oxide forgings can be classified into two distinct types: (1) brittle and (2) ductile. Forgings with oxygen contents above 600 ppm fractured with stable crack propagation, followed by unstable brittle fracture. On the other hand, forgings with lower oxide contents suggest a ductile type of fracture. Here stable crack propagation followed by fracture indicative of shear lip formation was evident. Therefore, a ductile/brittle fracture transition for P/M steel forgings is between 600 and 800 ppm oxide content. The relationship between oxygen content and fracture energy of P/M steel forgings is shown in figure 10. Extrapolation of the resultant curve shows that the ductile/brittle transition is approximately 650 ppm oxygen.

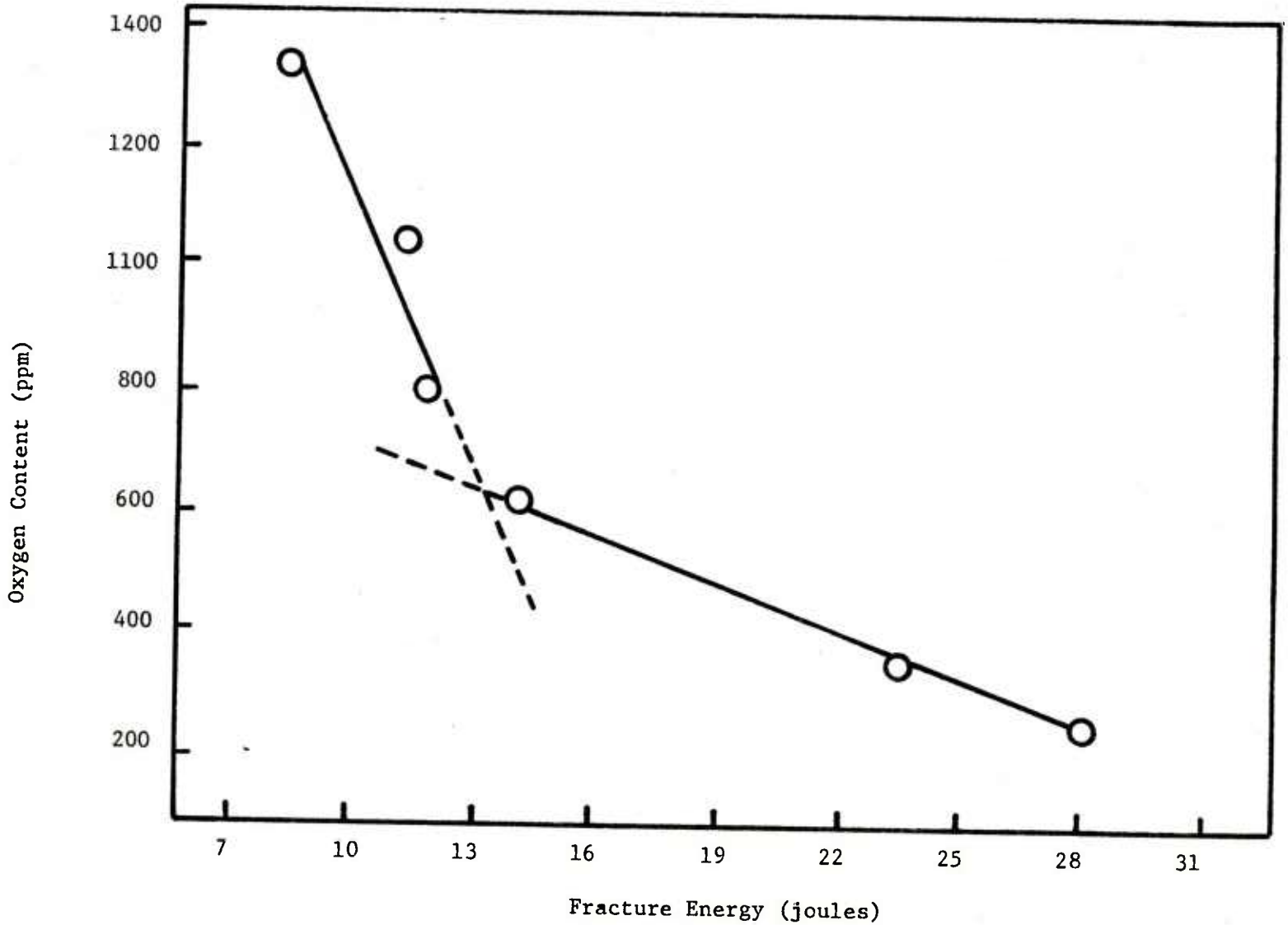

Figure 10. Fracture energy of P/M steel forgings as a function of oxygen content.

CONCLUSIONS

Military Specification MIL-F-45961 (see Appendix) covers forged metal parts fabricated from 4600 modified, prealloyed powder plus blended carbon. The successful application of the powder metallurgy forging process to ordnance components depends on meeting the property requirements of this specification. The results of this study have shown that only through careful control of the final oxide content can acceptable dynamic properties be obtained. The final oxide content is in turn determined by the sintering step of the P/M forging process. Most of the harmful oxides can be reduced at 1200°C under a variety of sintering atmospheres (reducing, inert, or vacuum) provided the furnace dew point is sufficiently low for thermodynamic stability. The oxide content of manganese is quite difficult to reduce below 1200°C and can adversely affect the P/M steel forging properties. Sintering at higher temperatures (1260°C and 1315°C) over a longer period of time can substantially reduce the amount of these oxides. However, operational and equipment costs for this type of sintering process can be quite expensive.

The fracture behavior of P/M steel forgings is also dependent upon the oxide content. High-oxide forgings fracture in a brittle manner and have low fracture toughness values. Low-oxide forgings fracture in a ductile manner and have characteristically higher fracture toughness values. A ductile/brittle fracture criterion dependent upon oxide content in P/M forgings has been postulated. Ductile fracture predominates when the oxide content is below 650 ppm, whereas brittle fracture prevails when the oxide content is above 650 ppm.

FUTURE WORK

Future efforts will be directed toward establishing the influence of surface porosity and preform density on the mechanical properties of parts forged from prealloyed 4600 steel powder. Variables to be investigated in the surface porosity study will include die temperature, forging pressure, and lateral deformation. Fatigue/surface porosity relationships will be determined by use of controlled surface porosity forgings and fracture mechanics. The preform density investigation will include novel alternate preforming operations such as loose-bag or "pack-sintering" compaction. The effect of preform density will be determined on the basis of the forging's final density, impact energy, and homogeneity, and purity of microstructure.

REFERENCES

1. M. J. Koczak, C. L. Downey, and H. A. Kuhn, "Structure/Property Correlations of Aluminum and Nickel Steel Preform Forgings," Powder Metallurgy International, Vol. 6, No. 1, 1974, p 13-16.

2. G. W. Cull, "Mechanical and Metallurgical Properties of Powder Forgings," Powder Metallurgy, Vol. 13, No. 26, 1970, p 156-164.

3. F. T. Lally, I. J. Toth, and J. DiBenedetto, "Forged Metal Powder Products," SWERR-TR-72-51, Rock Island Arsenal, Rock Island, IL, August 1972.

4. G. T. Brown and T. B. Smith, "The Relevance of Traditional Materials Specifications to Powder Metal Products," Modern Developments in Powder Metallurgy, Plenum Press, NY, 1974, Vol. 7, p 9-31.

5. H. A. Kuhn, M. M. Hagerty, H. L. Gaigher, and A. Lawley, "Deformation Characteristics of Iron-Powder Compacts," Modern Developments in Powder Metallurgy, Plenum Press, NY, 1971, Vol. 4, p 463-473.

6. A. Joshi, J. Wildermuth, and D. G. Stein, "Effect of Impurity Elements on the Properties of Iron P/M Compacts," The International Journal of Powder Metallurgy and Powder Technology, Vol. 11, No. 2, 1975, p 137-142.

7. J. P. Cook, Oxidation, Reduction, and Decarburization of Metal Powder Preforms, Hoeganaes Corporation, Riverton, NJ 1972.

8. A. Crowson and F. E. Anderson, "Properties of Powder Metallurgy Steel Forgings," presented at 1977 National Powder Metallurgy Conference, 1977, in press.

9. R. M. Pilliar, W. J. Bratina, and J. T. McGrath, "Fracture Toughness Evaluation of Powder-Forged Parts," Modern Developments in Powder Metallurgy, Plenum Press, NY, 1974, Vol. 7, p 51-72.

10. C. Durdaller, Furnace Atmospheres, Hoeganaes Corporation, Riverton, NJ 1971.

11. P. Lindskog, Unpublished Research, Hoganas AB.

12. P. Lindskog and S. E. Grek, "Reduction of Oxide Inclusions in Powder Preforms Prior to Hot Forming," Modern Developments in Powder Metallurgy, Vol. 7, 1973, p 185-301.

13. D. R. Ireland, "Dynamic Properties of Superalloys at Elevated Temperatures," work conducted under WECOM Contract DAAFO3-71-C-0016, March 1971.

14. R. A. Wullaert, "Applications of the Instrumented Charpy Impact Test," Impact Testing of Metals, ASTM STP466, American Society for Testing and Materials, 1970, p 148-164.

15. A. A. Wells, "Application of Fracture Mechanics at and Beyond General Yielding," British Welding Journal, November, 1963.

APPENDIX. MILITARY SPECIFICATION (MIL-F-45961) FORGINGS, PREALLOYED STEEL POWDER

This specification is approved for use by all Departments and Agencies of the Department of Defense.

Scope

This specification covers forged metal powder parts fabricated from 4600 (Modified) prealloyed powder plus blended carbon.

Applicable Documents

The following documents, of the issue in effect on date of invitation for bids or request for proposal, form a part of this specification to the extent specified herein.

Standards

Federal

Fed. Test Method Std. No. 151 - Metals; Test Methods

American Society for Testing and Materials

ASTM Standard Test Method B-328

(Copies of specifications, standards, drawings and publications required by suppliers in connection with specific procurement functions should be obtained from the procuring activity or as directed by the contracting officer.)

Requirements

Chemical composition. The forged metal powder parts, and the mechanical test specimens, shall conform to the requirements of Table A-1. The parts and test specimens shall be fabricated from 4600 (Modified) pre-alloyed powder plus blended carbon.

Table A-1. Chemical composition

Element	Analysis (Percent)
Carbon	0.38 - 0.43
Nickel	1.65 - 2.00
Molybdenum	0.4 - 0.6
Manganese	0.15 - 0.30
Phosphorus	0.04 (max.)
Sulfur	0.04 (max.)
Oxygen	0.030 (max.)
Silicon	0.35 (max.)

Mechanical Properties

The mechanical properties, at room temperature, of the austenitized, quenched, and tempered test specimens representing the metal powder parts shall conform to Table A-2.

Table A-2. Mechanical properties (minimum)

Yield Strength[1] (ksi)	Tensile Strength (ksi)	Elongation[2] (Percent)	Reduction of area (Percent)	Impact Strength[3,4] (Ft. lbs.)	Hardness[5] (Rockwell-C)
110	130	10.0	35.0	25 @ +72°F 8 @ -70°F	30-33

1. 0.2% offset
2. 2" gage length
3. Charpy V-notch
4. Specified temperatures have a tolerance range of $\pm 2^{\circ}F$
5. Although the drawing or requirement for a particular part may specify different hardness levels, the test specimens, and only the test specimens, shall be heat treated to the hardness specified in this table.

Density

The density of the parts and the test specimens shall be at least 7.81 g/cc. The density of sample specimens taken from the part shall be at least 7.80 g/cc.

Decarburization

Unless otherwise specified, surface decarburization, total and partial, of the parts and the test specimens shall not exceed 0.001 inch.

Microstructure

The microstructure of the quenched and tempered parts and test specimens shall be the same and exhibit homogeneity equal to or better than figure A-1. Figure A-2 is a representative example of unacceptable microstructure.

Figure A-1. Etchant: 2% Nital. Mag: 100X

Figure A-2. Etchant: 2% Nital. Mag: 100X

DISTRIBUTION LIST

Director
Defense Research and Engineering Office
ATTN: DDRE (R&AT)
Washington, DC 20310

Director
Defense Advanced Research Projects Agency
ATTN: Dr. E. Van Redth
1400 Wilson Boulevard
Arlington, VA 22209

Defense Documentation Center (12)
Cameron Station
Alexandria, VA 22314

Commander
US Army Armament Research and Development Command
ATTN: DRDAR-TDR
DRDAR-SC
DRDAR-SCP
DRDAR-SCM (10)
DRDAR-SCM-P
DRDAR-SCM-M
DRDAR-LC
DRDAR-LCU
DRDAR-TSS
DRDAR-QA
DRCPM-CAWS
DRCPM-SA
DRCPM-ADG
DRCPM-NUC
DRCPM-AAH 30 mm
DRCPM-TMA
Dover, NJ 07801

Assistant Secretary of the Army (R&D)
ATTN: Deputy for Science and Technology
Washington, DC 20310

Deputy Chief of Staff for Research,
Development and Acquisition
Department of the Army
ATTN: DAMA-ARZ-D
Washington, DC 20310

Commander
US Army Materiel Development and Readiness Command
ATTN: DRCMT
DRCDM-D
DRCDM-R
DRCDE-E
DRCDE-I
DRCDE-W
5001 Eisenhower Avenue
Alexandria, VA 22333

Commander
US Army Materials and Mechanics Research Center
ATTN: DRXMR, Dr. E. Wright
DRXMR-PT
Watertown, MA 02172

Commander
US Army Tank-Automotive Materiel Readiness Command
ATTN: DRSTA-E
Warren, MI 48090

Commander
US Army Electronics Research and Development Command
ATTN: DRSEL (Tech Lib)
Fort Monmouth, NJ 07703

Commander
US Army Missile Research and Development Command
ATTN: Technical Library
Huntsville, AL 35809

Commander
US Army Troop Support and Aviation
Materiel Readiness Command
ATTN: DRSTS
4300 Goodfellow Boulevard
St. Louis, MO 63120

Commander
US Army Aviation Research and Development Command
ATTN: DRDAV-EXT (Tech Lib)
P.O. Box 209
St. Louis, MO 63166

Director
US Army Mobility Equipment Research and
Development Command
ATTN: DRDME-MMM
Fort Belvoir, VA 22060

Director
US Army Advanced Materials Concept Agency
ATTN: Technical Library
2471 Eisenhower Avenue
Alexandria, VA 22314

Director
US Army Industrial Base Engineering Activity (2)
ATTN: DRXIB-MT
Rock Island, IL 61201

Commander
US Army Research and Standardization Group (Europe)
ATTN: DRXSN-E-RM
P.O. Box 65
FPO, New York 04510

Commander
US Army Foreign Science and Technology Center
ATTN: Mr. W. F. Marley
220 Seventh Street, N.E.
Charlottesville, VA 22901

Commander
US Army Research Office
ATTN: Metallurgy & Materials Science Division,
Dr. G. Mayer, Director
P.O. Box 12211
Research Triangle Park, NC 27709

Director
Ballistic Research Laboratory
ATTN: DRDAR-BLT
Aberdeen Proving Ground, MD 21010

Director
Harry Diamond Laboratories
ATTN: DRXDO-TIA
2800 Powder Mill Road
Adelphi, MD 20783

Director
National Bureau of Standards
ATTN: Technical Library
Washington, DC 20025

Metals and Ceramic Information Center
Battelle Memorial Institute
505 King Avenue
Columbus, OH 43201

Weapon System Concept Team/CSL
ATTN: DRDAR-ACW
Aberdeen Proving Ground, MD 21010

Technical Library
ATTN: DRDAR-CLJ-L
Aberdeen Proving Ground, MD 21010

Technical Library
ATTN: DRDAR-TSB-S
Aberdeen Proving Ground, MD 21005

Benet Weapons Laboratory
Technical Library
ATTN: DRDAR-LCB-TL
Watervliet, NY 12189

Commander
U.S. Army Armament Materiel Readiness Command
ATTN: DRSAR-LEP-L
Rock Island, IL 61299

U.S. Army Materiel Systems Analysis Activity
ATTN: DRXSY-MP
Aberdeen Proving Ground, MD 21005

Director
US Army Natick Research and Development Command
ATTN: Technical Library
Kansas Street
Natick, MA 07160